Theor Chem Acc (2009) 124:115–122
DOI 10.1007/s00214-009-0588-y

REGULAR ARTICLE

Interaction between uracil nucleobase and phenylalanine amino acid: the role of sodium cation in stacking

**Ali Ebrahimi · Mostafa Habibi-Khorassani ·
Ali Reza Gholipour · Hamid Reza Masoodi**

Received: 29 January 2009 / Accepted: 12 May 2009 / Published online: 29 May 2009

Abstract The stacking interactions in the uracil:phenylalanine (U:PHE) and (U:PHE)···Na^+ complexes have been studied at different levels of theory, in which the structures were optimized by both standard and gradient counterpoise corrected methods. The Na^+ cation can interact with different sites of stacked U:PHE unit. The geometrical parameters of the optimized structures and the calculated binding energies reveal the influence of cation interaction on π–π stacking and vice versa. The interplay between π–π stacking and cation interaction has also been investigated by topological analysis of electron charge density using atoms in molecules (AIM) method. A good agreement between the results of AIM analysis and calculated binding energies has been observed in dimer and complexes.

Keywords Intermolecular interaction · Atoms in molecules · Ab initio · Cation interaction · Cooperativity

1 Introduction

Intermolecular interactions between aromatic systems have been studied during the past two decades, by both experimental [1, 2] and theoretical methods [3–13]. Among these interactions, the importance of the π–π interactions has been repeatedly stressed in many fields of chemistry and biochemistry [14–17]. For example, the π–π stacking interactions play a controlling role in the enzyme-nucleic acid recognition regulating gene expression, intercalation of drugs with DNA, and so on. For this reason, the stacking interactions were, and still are the subject of numerous works [18–23]. Theoretical methods can be used to characterize weak interactions between amino acids and/or nucleobases, and to correctly determine the structure of π–π stacked systems that are essential for the further applications of these functionals to the systems of biological interest. Unfortunately, theoretical study on a π–π interaction is a difficult task and requires the use of very sophisticated and accurate methods [8, 9, 24, 25]. On the other hand, the great majority of these studies have involved the interactions of aromatic systems with alkali metal cations, particularly Na^+ and K^+, mainly because these cations are very common in organisms and are the most biologically relevant metal cations [26–32]. These interactions are important in the regulation of enzymes and the stability of large RNA molecules and proteins [33]. They are also important for the binding of acetylcholine to the active site of the enzyme acetylcholine esterase and recently, their importance has been demonstrated to neurotransmitter receptor [34, 35].

The two NH bonds in uracil (U) biologically affect its hydrogen bonding capability as well as the activity of enzymes for which the U is a substrate. On the other hand, enormous efforts have been made to exploit RNA as a drug target [36]. In the present work, the U (with two NH acid groups) and the PHE (which is modeled by a benzene ring) compounds and Na^+ cation have been selected to investigate the interplay of two primary non-covalent interactions, namely metal cation–π interaction and π–π interaction. Thus, the results of calculations for uracil:phenylalanine (U:PHE) dimer have been compared with those of PHE:U···Na^+ (**T1** and **T2**), U:PHE···Na^+ (**T3**), U···Na^+ (**D1** and **D2**), and PHE···Na^+ (**D3**) complexes. The effect

---

A. Ebrahimi (✉) · M. Habibi-Khorassani ·
A. R. Gholipour · H. R. Masoodi
Department of Chemistry, University of Sistan and Baluchestan,
P.O. Box 98135-674, Zahedan, Iran
e-mail: ebrahimi@hamoon.usb.ac.ir

of counterpoise correction (CP) on geometries and energy values has also been considered at several levels of theory.

2 Computational methods

Theoretical studies on stacking interaction between the natural nucleobases and aromatic amino acids [8, 9, 25] have shown that the stacking energy is highly sensitive to the method and basis set, which is referred to dispersion interactions [37]. Thus, any ab initio quantum mechanical modeling of a non-covalent interaction, that ought to include a description of electron correlation, has to capture the dispersion interaction. This can be accomplished most easily by using the second-order Møller–Plesset perturbation theory [38].

Hobza and Sponer [12, 17] have carefully outlined suitable computational approaches for studying these interactions. Generally, attempts to fully optimize stacked geometries led to hydrogen-bonded arrangements, which were in part due to the absence of basis set superposition error (BSSE) correction in the routine optimization [8, 39]. Furthermore, distortions in the monomer geometries were often seen in attempts to fully optimize the stacked dimers.

In nucleobase model (U), the sugar–phosphate RNA backbone was replaced with a hydrogen atom. Similarly, the amino acid residue was obtained by the replacement of its protein backbone with a hydrogen atom (PHE). This reduced PHE structure to benzene, in which only aromatic part was taken for PHE. Model compounds were fully optimized preserving planarity (C_s symmetry) at MP2/6-31G** level of theory.

The approximate geometries and bending energies of some stacked dimers including U:PHE have previously been studied using freeze scan of distances and angles by Wetmore et al. [9]. In this work, three dihedral angels were fixed between two rings in the geometry optimization of dimer and hereunder mentioned complexes. The geometries have been optimized using the standard and the gradient CP-corrected methods, which in latter the BSSE is estimated during the process.

MP2 is the most commonly used and computationally tractable method of describing dynamic electron correlation, which is ultimately the source of dispersion forces. The π–π stacking energies have extensively been studied at the different levels of theory, which includes the MP2 method with a special but relatively small basis set 6-31G*(0.25) [12]. Unfortunately, this method is known to consistently overestimate binding energies in the stacked nucleic acid base pairs. Also, MP2 calculations are too expensive for detailed of typical systems of stacked nucleic acid base pairs. Nevertheless, in order to compare the results of full optimization with those of freeze scan [9], the calculations have been performed by MP2 method with different basis sets.

On the other hand, density functional theory (DFT) is an important tool for studying biological systems [40–48]. However, the most popular DFT method, B3LYP, cannot describe stacking interactions because B3LYP fails badly for dispersion interactions. The new functionals of M05 and M06 families of Zhao and Truhlar [49–51] seem to offer the promise of good performance for π–π stacking energies [40–45].

Single-point calculation has been performed for the dimer and the complexes at MP2/6-31G*(0.25) level of theory, in which the standard d-exponent 0.85 of basis set is replaced by 0.25 for the second row atoms. It seems to be a more adequate basis set for selected systems due to the addition of diffuse-polarization function, which has been shown to yield more accurate values of the correlation contribution to stacking interaction [52]. All mentioned calculations have been performed by using Gaussian 03 program package [53]. The geometry optimization of the dimer and the complexes have also been performed at M05-2X/6-31G** level of theory within GAMESS program [54].

The wave functions obtained at MP2/6-31G** level of theory have been analyzed by the quantum theory of atoms in molecules QTAIM [55] using AIM2000 software [56].

It is comfortable to describe the geometries with the centriod–centriod distance R_{cen}, the shortest distance between two carbons R_{clo}, and the interplanar angle γ. R_{cen} and R_{clo} used in order to determine both horizontal and vertical displacements of both fragments (see Scheme 1).

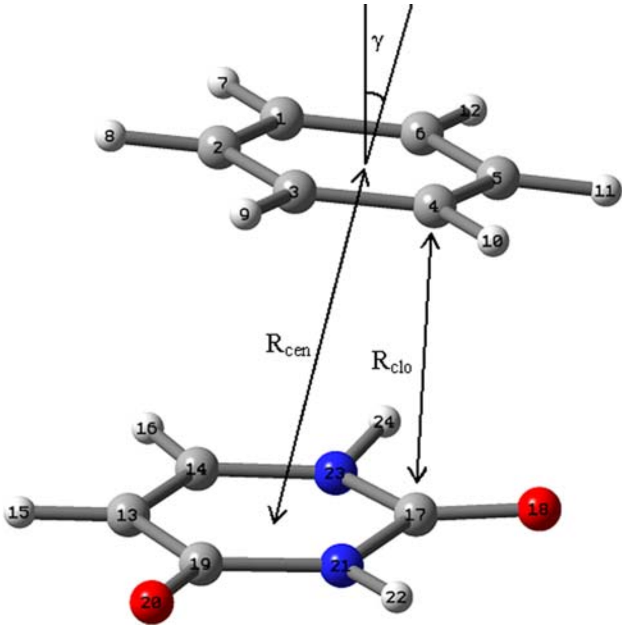

Scheme 1 Most important parameters used for identification of geometries. The distances are in Å and angles are in degrees

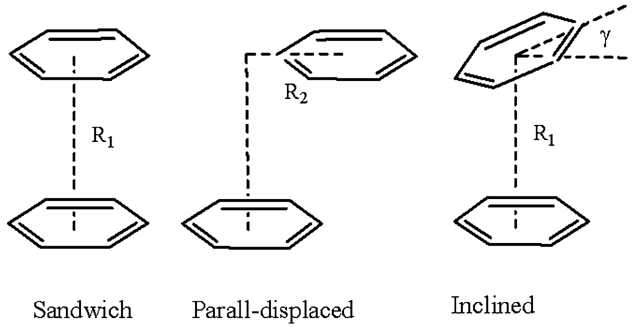

Scheme 2 The description of the Sandwich, parallel-displaced and inclined configurations

Sandwich, parallel-displaced and inclined configurations can be defined in respect to those parameters (see Scheme 2). In the sandwich configuration, one ring places on the top of the other. Parallel-displaced configuration is reached from the sandwich configuration by a parallel shift of one ring away from the other (horizontal displacement, R2), and inclined configuration is made from a parallel-displaced configuration by a γ-degree inclination of a ring (see Scheme 2).

To optimize the structures at MP2/6-31G** level of theory, the sandwich configuration was selected for dimer and complexes, in which the U has been placed over the PHE at a distance of 4.5 Å (R_{cen}).

Several M–π–π complexes were designed by considering various orientations of Na^+ with respect to U:PHE dimer. The Na^+ cation has been placed near the O_{18} and O_{20} atoms of the U in the complexes **T1** and **T2,** respectively, and above the center of benzene ring in the complex **T3** (see Fig. 1).

3 Results and discussion

The most important geometrical parameters of dimer and complexes optimized at MP2/6-31G** level of theory by using standard and CP-corrected methods are listed in Table 1. As can be seen, geometrical parameters R_{cen}, R_{clo} and γ for the U:PHE dimer are equal to 3.614, 3.146 Å and 24.90°, respectively, using standard method. R_{clo} is the distance between the C4 and C17 atoms (see Scheme 1). The values of R_{cen} and γ values were previously obtained as 3.50 Å and 0.0° by freeze scan at MP2/6-31G*(0.25) level of theory [9]. The optimized horizontal displacement of two fragments is larger and the vertical displacement of them is smaller than the previous results.

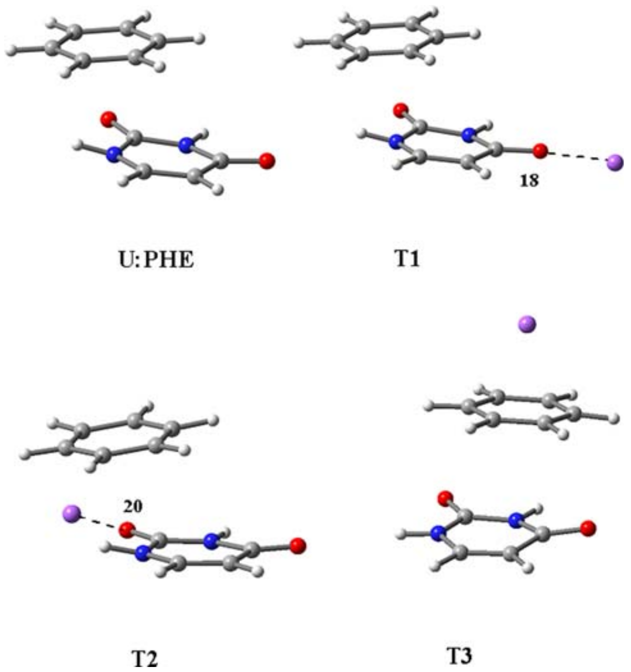

Fig. 1 Optimized geometries at MP2/6-31G** level of theory for dimer and complexes **T1**–**T3**

Table 1 The most important optimized geometrical parameters (in Å and degrees)

Compound	R_{ca}	R_{cen}	R_{clo}	γ
MP2/6-31G**, standard method				
U:PHE	–	3.614	3.146	24.91
T1	2.120 (2.129)	3.554	3.141	24.25
T2	2.117 (2.137)	3.574	3.141	26.24
T3	2.381 (2.391)	3.483	3.137	19.43
MP2/6-31G**, CP-corrected method				
U:PHE	–	3.890	3.418	24.77
T1	2.190	3.629	3.155	23.27
T2	2.139	3.878	3.488	23.41
M05-2X/6-31G**, standard method				
U:PHE	–	3.473	3.350	4.00
T1	2.079	3.486	3.50	0.00
T2	2.086	3.483	3.339	0.00
M06-2X/6-31G**, standard method				
U:PHE	–	3.361	3.295	4.41
T1	2.061	3.416	3.322	1.81
T2	2.077	3.394	3.316	1.32

The data in the parentheses correspond to dimers **D1**–**D3**

In addition, the geometrical parameters of the dimer have been optimized by using CP-corrected method at MP2/6-31G** level of theory. The optimized parameters R_{cen}, R_{clo} and γ are equal to 3.90, 3.41 Å and 24.77°, respectively. The R_{cen} and R_{clo} distances in the CP-corrected method are larger than those in the standard method.

The effect of sodium cation on the U:PHE dimer has also been investigated at MP2/6-31G** level of theory by both standard and gradient CP-corrected methods. The geometries of the complexes **T1–T3** have been fully optimized at the mentioned level. An additional geometrical parameter, the distance between Na^+ and ring (R_{ca}), is needed to specify the optimized structures of these complexes.

As can be seen in Table 1, the trend in the optimized values for R_{cen}, R_{clo}, and γ is **T3** < **T1** < **T2**. As a result, the Na^+ cation has a higher effect on stacking when interact with π system of the PHE ring (in the complex **T3**). The deviations of geometrical parameters from the optimized parameters in the U:PHE dimer are higher than those in the complex **T3**. The values of R_{clo} reported in Table 1 correspond to the distance between C4 and C17 in the complexes **T1** and **T2** and the distance between C2 and C19 in the complex **T3.** All mentioned optimized geometrical parameters in complexes are lower than those in dimer (with the exception of γ in **T2**). Thus, the stacking interaction can be enhanced by the cation interaction.

The optimized value for R_{ca} is equal to 2.120, 2.117 and 2.380 Å in the complexes **T1**, **T2** and **T3**, respectively. This parameter is equal to 2.129, 2.137 and 2.390 Å in the dimers **D1**, **D2** and **D3**, respectively. The distance between the Na^+ cation and ring is shortened by stacking interaction so that the cation interaction is enhanced by the stacking interaction in all complexes.

The geometries of the complexes **T1** and **T2** have also been optimized by using CP-corrected method at MP2/6-31G** level of theory. The optimized parameters R_{cen}, R_{clo}, R_{ca} and γ, respectively, are equal to 3.628, 3.155, 2.190 Å and 23.27° in the complex **T1** and 3.878, 3.487, 2.138 Å and 23.41° in the complex **T2**. With the exception of γ, which has a slight decrease, the referred parameters increase when CP-correction is made in optimization.

The geometry optimization has also been performed at M05-2X/6-31G** and M06-2X/6-31G** levels of theory for dimer and complexes. For the U:PHE dimer, the horizontal displacement of two fragments decreased by 0.141 and 0.253 Å, vertical displacement of them increased by 0.20 and 0.05 Å, and interplanar angle decreased by 20.91 and 20.41°, when the method changed from MP2 to M05-2X and M06-2X, respectively. The results of full geometry optimization of complexes **T1** and **T2** using M05-2X and M06-2X methods are summarized in Table 1. Two rings are perfectly parallel in complex **T1** and are roughly parallel in complex **T2** at those levels. The values of R_{cen}, R_{clo}, and R_{ca} parameters change by 0.068–0.180, −0.181 to −0.359, 0.031–0.059 Å, respectively, when the method change from MP2 to M05-2X and M06-2X. Hence, the horizontal displacement is smaller for mentioned DFT functionals. By these methods, the geometry optimization of the complex **T3** did not succeed due to convergence problem.

The calculated binding energies at different levels of theory are given in Table 2. As shown in this table, the stacking energy calculated for the dimer at MP2/6-31G** level of theory equals −27.32 kJ mol^{-1} without BSSE correction. This value at MP2/6-31G*(0.25) level of theory is equal to −68.50 kJ mol^{-1}. The binding energy increases by −41.18 kJ mol^{-1} with a change in basis set from 6-31G** to 6-31G*(0.25), which increases the interactions with *d* orbitals.

Furthermore, the binding energies have been corrected for BSSE by using the Boys–Bernadi counterpoise technique [57] for standard structures optimized at MP2/6-31G** level. The CP-corrected values at MP2/6-31G** and MP2/6-31G*(0.25) levels of theory are equal to −10.19 and −26.02 kJ mol^{-1}. The BSSE correction decreases the interaction energy by 62%, which is high in comparison with regular hydrogen bonds. The binding energy has previously been calculated to be −20.1 kJ mol^{-1} using freeze scan at MP2/6-31G*(0.25) level by Wetmore et al. [9] and −26.19 kJ mol^{-1} using partial optimization at MP2/aug-cc-PVDZ level by Cysewski [25] (the binding energy for optimized dimer in this work at MP2/aug-cc-PVDZ level is equal to −27.04 kJ mol^{-1}). Thus, the geometry optimization increases the binding energy by 5.92 kJ mol^{-1} (see Table 2).

As a result, the π–π staking interaction energy is equal to −12.99 kJ mol^{-1} for the structure optimized by using

Table 2 The binding energies (multiplied by a negative sign) calculated by MP2 method for dimers and complexes in kJ mol^{-1}

	MP2/6-31G**	MP2/6-311 ++G**	MP2/6-31G*(0.25)	M06-2X/6-31G**
U:PHE	27.31, *10.19*, **12.99**	43.15, *21.68*	68.50, *26.02*	24.74 (17.82)
T1	194.92, *161.63*, **164.21**	190.92, *164.95*	235.18, *178.86*	198.96 (193.11)
T2	182.41, *149.21*, **151.86**	176.40, *150.67*	221.45, *167.91*	183.67 (177.98)
T3	157.96, **113.27**	149.83, *114.17*	199.26, *133.52*	
D1	159.38, **144.15**	140.03, *136.34*		
D2	145.70, **130.92**	127.29, *123.14*		
D3	119.89, **99.02**	99.14, *87.58*		

The italicized data corrected for BSSE. The bold data in the second column correspond to gradient CP-corrected structures. The data in the parentheses correspond to M05-2X functional gradient CP-corrected method at MP2/6-31G** level. Although the stacking energy in standard structure without BSSE correction is higher in comparison with that in the optimized structure with CP-corrected method, it becomes lower with that correction.

However, the binding energies of the complexes **T1–T3** calculated at different levels of theory are gathered in Table 2. The additive behavior of cation interaction on the stacking and vice versa can be observed with regard to ΔE values. The binding energies for standard structures of the complexes **T1–T3** calculated at MP2/6-31G** level without BSSE correction are equal to −194.93, −182.41 and −157.97 kJ mol^{-1}, respectively, such that $\Delta E_1 > \Delta E_2 > \Delta E_3$. Those values are higher than the sum of ΔE(**D1**, **D2** or **D3**) and ΔE(U:PHE) that are equal to −186.70, −173.02 and −147.21 kJ mol^{-1} for the complexes **T1**–**T3**, respectively. The differences can be attributed to the additive behavior of cation interactions in the complexes. The enhancement of both U···Na^{+} (or PHE···Na^{+}) and U:PHE interactions can be observed when consulted with the geometrical parameters of complexes, in which the units become closer in the complexes **T1–T3**. Thus, the difference between the ΔE values can be attributed to the different interactions between Na^{+} and rings, and to the different enhancement of the π–π stacking in the presence of different ring···Na^{+} interactions. The minimum and maximum values correspond to the complexes **T3** and **T1**, respectively. In order to study the effect of basis set on interaction energies, they have also been computed at the MP2/6-31G*(0.25) level. At this level, the interaction energy for the complexes **T1–T3** is equal to −235.18, −221.45 and −199.26 kJ mol^{-1}, respectively. As can be seen, the values are higher than those calculated at MP2/6-31G** level of theory.

To develop the results, the interaction energies calculated with the extended basis set have also been corrected for BSSE. The corrected binding energies for the complexes **T1–T3** are equals to −178.86, −167.91 and −133.52 kJ mol^{-1}**,** respectively. In this way, the binding energies decrease by 56.32, 53.54 and 65.74 kJ mol^{-1} in the complexes **T1–T3**, respectively. The binding energies calculated for CP-corrected structures of the complexes **T1** and **T2** at MP2/6-31G** level are equal to −161.21 and −151.8 kJ mol^{-1}, respectively. The geometry optimization of the complex **T3** with the gradient CP-corrected method did not succeed due to convergence problem. In addition, the binding energies have been calculated at MP2/6-311++G** level of theory (see Table 2). Lower interaction energies have been obtained with 6-311++G** in comparison with 6-31G*(0.25) basis set. Although the calculated binding energies with 6-311++G** basis set are lower than calculated values with 6-31G** basis set without BSSE correction (for the complexes **T1–T3**), but the order is reversed with that correction.

The binding energies for standard structure of U:PHE dimer and complexes **T1** and **T2** calculated at M05-2X/6-31G** and M06-2X/6-31G** levels without BSSE correction are gathered in Table 2. The binding energy of dimer decreases by 9.5 and 34.8% when the method change from MP2 to M05-2X and M06-2X, respectively. The binding energy of complexes **T2** and **T3** change only 0.93 and 2.43% (or −2.17 and −0.69%) when the method change from MP2 to M05-2X (or M06-2X).

The topological analysis of electron charge density has been performed by AIM method on the wave functions obtained at MP2/6-31G** level of theory. As shown in molecular graphs of Fig. 2, a common feature of the dimer and the complexes is the formation of bond critical points (BCPs), ring critical points (RCPs) and cage critical points (CCPs) between U and PHE units. Small red spheres, small yellow spheres, small green spheres, and lines correspond to BCPs, RCPs, CCPs and bond paths, respectively.

The AIM data can be taken as indices to judge the strength of π–π stacking, and other intermolecular interactions [13, 29]. In each complex, BCPs locate along the lines connecting an atom of a ring to an atom of the other ring and the line connecting Na^{+} cation to a ring. Intermolecular BCPs observed between U and PHE rings correspond to C···C, C···O and C···N interactions.

With respect to the molecular graphs in Fig. 2, there are three intermolecular BCPs in the dimer and the complex **T2**, and four intermolecular BCPs in the complexes **T1** and **T3**. Three BCPs correspond to the C···C, C···O and C···N interaction in the dimer and the C···C, C···N and O···Na^{+} contacts in the complex **T2.** In addition to the C···C, C···N, and C···O BCPs, there is also a O···Na^{+} BCP in the complex **T1.** From four BCPs in the molecular graph of the complex **T3**, two BCPs link the O atoms of the U ring to the C atoms of the PHE ring, such that the corresponding bond paths substantially turn toward two vicinal C–C BCPs of the PHE ring, one BCP corresponds to the C···N interaction, and the other one corresponds to the C···Na^{+} interaction. The ρ and $\nabla^2\rho$ values calculated at intermolecular BCPs are reported in Table 3. The $\nabla^2\rho \times 10^2$ values calculated at intermolecular BCPs of dimer and complexes range from 2.05 to 2.82 au. If the classification of Rozas et al. [58] is correct for individual interactions in π–π stacking, with regard to $\nabla^2\rho > 0$ and $H_{\mathrm{BCP}} < 0$ at BCPs in the dimer and the complexes, they will classify as medium interactions. The comparison of the strength of interactions is difficult by evaluation of individual BCPs. We added the values of ρ calculated at intermolecular BCPs, $\Sigma\rho$, to obtain a measure for comparing stacking interactions. The values of $\Sigma\rho$ are equal to 21.642, 15.314, 19.968 and 22.870 × 10^{3} au in the dimer and the complexes **T1–T3**, respectively. Thus, the trend in $\Sigma\rho$ is **T3** > dimer > **T2** > **T1**. As previously mentioned, the

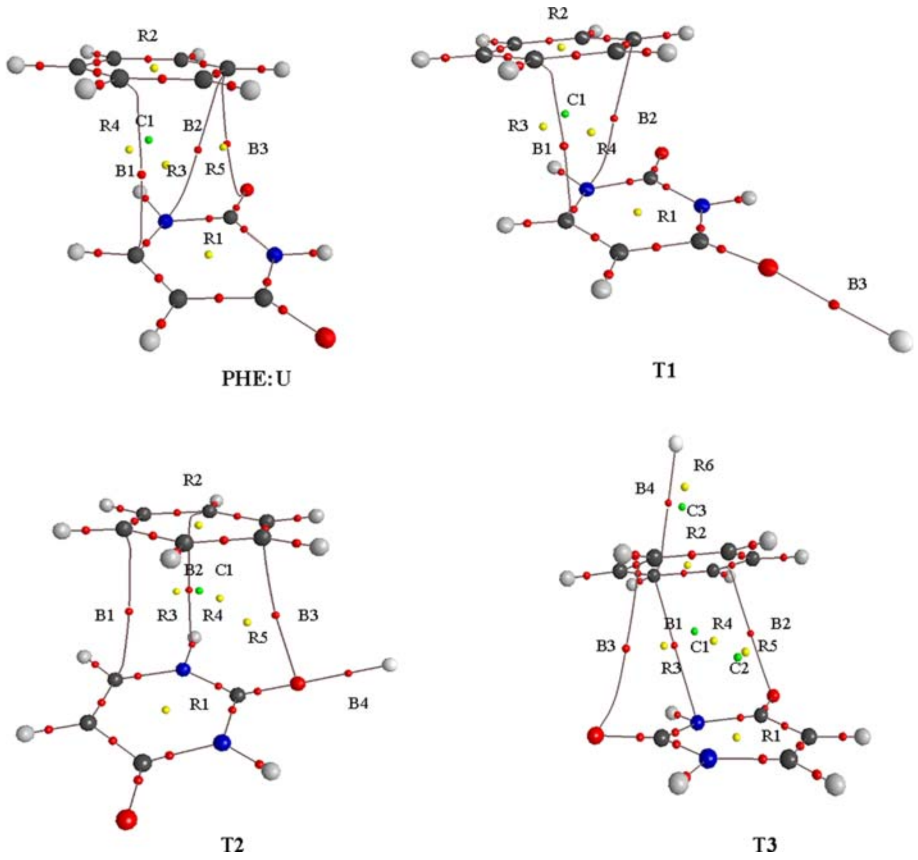

Fig. 2 The molecular graphs for dimer and complexes obtained using AIM analysis. *Small red spheres*, *small yellow spheres*, and *lines* represent bond critical points (BCP), ring critical points (RCP) and bond paths, respectively

trend in R_{cen} is dimer (3.614) > **T2** (3.554) > **T1** (3.574) > **T3** (3.483). The $\Sigma\rho$ index is not in agreement with the mentioned geometrical parameter in stacked structures**.** We could not take more than one BCP (C4···Na$^+$) between Na$^+$ and the C atoms of PHE in the complex **T3**. In addition, the $\rho \times 10^3$ (and $\nabla^2\rho \times 10^2$) values calculated at Na$^+$···ring are equal to 29.21 (23.65), 29.10 (23.75) and 11.44 (5.460) au in the complexes **T1**–**T3**, respectively. The values are higher in comparison with the ρ and $\nabla^2\rho$ values calculated at the intermolecular BCPs of dimers **D1**–**D3**.

Although the Na$^+$···ring interaction is expected to be stronger in the complex **T1**, it has a higher effect on π–π stacking interaction in the complex **T3**, in which the Na$^+$···π interaction occurs between Na$^+$ cation and PHE.

It is necessary to remember that the existence of CCP correlates with the phenomenon of stacking interaction [29]. Only one CCP is observed in the molecular graphs of the dimer and the complexes **T1** and **T2**, while two CCPs are observed in the complex **T3.** The values of ρ and $\nabla^2\rho$ at the CCPs of the complexes are higher than those in the dimer. The order of the ρ and $\nabla^2\rho$ values calculated at CCPs is **T3** (5.08, *2.24*) > **T1** (4.92, *2.19*) > **T2** (4.65, *2.07*) > dimer (4.65, *2.05*), which is in agreement with the order of parameters R_{cen} and R_{clo}. All ρ and $\nabla^2\rho$ (italicized data) values reported in atomic units and multiplied by 10^3 and 10^2, respectively. Although the trend in the values of $\Sigma\rho$ corresponding to intermolecular RCPs (18.596, 12.245, 17.221 and 22.337 × 10^3 au in the dimer and the complexes **T1**–**T3**, respectively) is not in agreement with the parameters R_{cen} and R_{clo} of stacked structures, but the trend in the higher values is **T3** > dimer > **T2** > **T1**. As can be seen in Table 3, the ρ (and $\nabla^2\rho$) values at the center of U and PHE rings in the U:PHE dimer are equal to 19.87 (16.37), and 19.06 au (15.54 au), respectively. These parameters in the U and the PHE are equal to 18.9 (15.37) and 19.75 (16.38), respectively. These results show that the formation of U:PHE dimer increases the ρ_{RCP} and $\nabla^2\rho_{\mathrm{RCP}}$ values at the center of PHE ring and decreases those at the center of U ring. The order of ρ (and $\nabla^2\rho$) values at the RCP of U is **T3** (18.95, *15.46*) < **T1** (19.50, *16.07*) < **T2** (19.87, *16.33*) ≈ dimer (19.87, *16.37*), which are higher than those at the center of an isolated U (18.90, *15.37*). The order at the RCP of PHE ring is **T3** (20.28, *16.22*) > **T1** (19.91, *16.36*) > **T2** (19.22, *15.71*) > dimer (19.06, *15.54*), which are higher or lower than those at the center of an isolated PHE (19.75, *16.38*). However, the value at the O···Na$^+$ BCP is equal to 29.21 (23.65) and 29.10 (23.75) in the complexes **T1** and **T2**, while it is equal to 28.42 (22.89) and 27.71 (22.19) in the complexes **D1** and **D2**, respectively. Also, the value at C···Na$^+$ BCP is equal to 11.44 (5.46) in the complex **T3**, whereas it is equal to 8.38 (4.37)

Table 3 Topological properties calculated at intermolecular BCPs and RCPs by using AIM method (in au, see Fig. 2 for nomenclature)

CP	ρ	$\nabla^2\rho$	CP	ρ	$\nabla^2\rho$	CP	ρ	$\nabla^2\rho$
U:PHE			*T2*			R4	6.007	1.992
B1 (C···C)	6.949	2.048	B1 (C···C)	7.405	2.355	R5	3.726	1.395
B2 (C···N)	7.492	2.281	B2 (C···N)	6.155	2.121	R6	10.667	5.157
B3 (C···O)	7.201	2.057	B3 (C···O)	6.407	2.161	C1	5.079	2.243
R1	19.869	16.368	B4 (O···Na^+)	29.1	23.75	C2	3.635	1.526
R2	19.063	15.536	R1	19.867	16.333	*PHE*		
R3	4.928	1.765	R2	19.215	15.707	R	19.746	16.375
R4	6.471	2.102	R3	6.117	2.087	U		
R5	7.196	2.755	R4	6.060	2.077	R	18.899	15.373
C1	4.651	2.045	R5	5.044	1.807	*D1*		
T1			C1	4.652	2.066	R	19.296	15.863
B1 (C···N)	7.624	2.266	*T3*			B (O···Na^+)	28.421	22.889
B2 (C···O)	7.691	2.389	B1 (C···N)	6.869	2.099	*D2*		
B3 (O···Na^+)	29.209	23.649	B2(O···BCP)	8.336	2.816	R	19.093	15.574
R1	19.499	16.075	B3(O···BCP)	7.663	2.696	B (O···Na^+)	27.714	22.185
R2	19.907	16.36	B4 (C···Na^+)	11.435	5.462	*D3*		
R3	5.396	1.863	R1	18.951	15.461	R	20.176	16.219
R4	6.849	2.197	R2	20.276	16.217	B	8.384	4.365
C1	4.924	2.189	R3	6.462	2.202			

The ρ and $\nabla^2\rho$ data multiplied by 10^3 and 10^2

in the complex **D3**. These results confirm a growth of the Na^+···ring interaction on the stacking.

In accord with the energy data, the comparison of ρ (and $\nabla^2\rho$) values calculated at BCPs, RCPs and CCPs of the dimers and the complexes show that π–π stacking and cation–ring interactions enhance each other.

4 Conclusions

The effect of basis set and BSSE correction on binding energies and also the effect of CP-correction on optimized geometries are actually important to the π–π stacking and cation–π interactions. The highest binding energy, with and without BSSE correction, corresponds to 6-31G*(0.25) basis set. In dimer, the binding energy calculated with 6-311++G** is higher than 6-31G**, with and without BSSE correction. On the other hand, the ΔE values calculated for the complexes with 6-31G** basis set are higher than those with 6-311++G** without BSSE correction, while the order is reversed with this correction. This correction decreases the ΔE values by 50–60% in the dimer and 15–30% in the complexes. The corrected binding energy for standard structure of the U:PHE dimer with extended basis set is $\Delta E_{\mathrm{cp}} = -26.02$ kJ mol^{-1}. The geometry optimization increases the binding energy approximately by 6 kJ mol^{-1} when compared with the result of Wetmore et al. [9], which has been calculated as a minimum on the energy surface by freeze scan. Optimization by gradient CP-corrected method at MP2/6-31G** level decreases the binding energy to -12.99 kJ mol^{-1}.

With 6-31G** basis set, changing the method from MP2 to M05-2X and M06-2X reduces the binding energy of dimer by 9.5 and 34.8%, respectively, while the changes are relatively small for complexes **T2** and **T3**.

The relationships between geometrical parameters R_{cen}, R_{clo} and γ cause the difference between optimized and scanned structures, and influence the binding energy. The Na^+ cation enhances the π–π stacking interaction for inclined configuration, and π–π stacking enhances the interaction between Na^+ and ring. The AIM analysis shows several intermolecular BCPs, RCPs and CCPs in the dimer and the complexes. All intermolecular BCPs are observed between two atoms of the U and the PHE rings, while in two cases the bond paths are substantially turned toward vicinal C–C BCPs. The best relationship is observed between ΔE and ρ (and $\nabla^2\rho$) values at CCPs.

References

1. Krause H, Ernstberger B, Neusser HJ (1991) Chem Phys Lett 184:411–417. doi:10.1016/0009-2614(91)80010-U
2. Neusser HJ, Krause H (1994) Chem Rev 94:1829–1843. doi:10.1021/cr00031a005
3. Van de Waal BW (1986) Chem Phys Lett 123:69–72. doi:10.1016/0009-2614(86)87017-8

4. Jorgensen WL, Severance DL (1990) J Am Chem Soc 112:4768–4774
5. Hobza P, Spirko V, Selzle HL, Schlag EW (1998) J Phys Chem A 102:2501–2504
6. Tsuzuki S, Honda K, Azumi R (2002) J Am Chem Soc 124:12200–12209
7. Gonzalez C, Lim EC (2000) J Phys Chem A 104:2953–2957
8. Rutledge LR, Campbell-Verduyn LS, Hunter KC, Wetmore SD (2006) J Phys Chem B 110:19652–19663
9. Rutledge LR, Campbell-Verduyn LS, Wetmore SD (2007) Chem Phys Lett 444:167–175
10. González Moa MJ, Mandado M, Mosquera RA (2007) J Phys Chem A 111:1998–2001
11. Mignon P, Loverix S, De Proft F, Geerlings P (2004) J Phys Chem A 108:6038–6044
12. Hobza P, Sponer J (1999) Chem Rev 99:3247–3276
13. Quiñonero D, Frontera A, Deyà PM, Alkorta I, Elguero J (2008) Chem Phys Lett 460:406–410. doi:10.1016/j.cplett.2008.06.028
14. Ranganathan D, Haridas V, Gilardi R, Karle IL (1998) J Am Chem Soc 120:10793–10800. doi:10.1021/ja982244d
15. Asakawa M, Ashton PR, Hayes W, Janssen HM, Meijer EW, Menzer S, Pasini D, Stoddart JF, White AJP, Williams DJ (1998) J Am Chem Soc 120:920–931
16. Biot C, Wintjens R, Rooman M (2004) J Am Chem Soc 126:6220–6221
17. Sponer J, Leszczynski J, Hobza P (2002) J Biopolymers 61:3–31. doi:10.1002/1097-0282(2001)61:1<3::AID-BIP10048>3.0.CO;2-4
18. Hunter AC, Sanders JKM (1990) J Am Chem Soc 112:5525–5534. doi:10.1021/ja00170a016
19. Hobza P, Selzle HL, Schlag EW (1993) J Phys Chem 97:3937–3938
20. Sponer J, Jurecka P, Hobza P (2004) J Am Chem Soc 126:10142–10151
21. Sponer J, Leszczynski J, Hobza P (1996) J Phys Chem 100:5590–5596
22. Gu J, Wang J, Leszczynski J, Xie Y, Schaefer HF (2008) Chem Phys Lett 459:164–166
23. Cysewski P, Czyznikowska Z, Zalesny R, Czelen P (2008) Phys Chem Chem Phys 10:2665–2672. doi:10.1039/b718635e
24. Czyżnikowska Ż, Zaleśny R, Ziółkowski M, Gora RW, Cysewski P (2007) Chem Phys Lett 450:132–137. doi:10.1016/j.cplett.2007.10.106
25. Cysewski P (2008) Phys Chem Chem Phys 10:2636–2645. doi:10.1039/b718394a
26. Dunbar RC (2000) J Phys Chem A 104:8067–8074. doi:10.1021/jp000524l
27. Ma JC, Dougherty DA (1997) Chem Rev 97:1303–1324
28. Gallivan JP, Dougherty DA (1999) Proc Natl Acad Sci 96:9459–9464
29. Zhikol OA, Shishkin OV, Lyssenko KA, Leszczynski J (2005) J Chem Phys 122:144104-1–144104-8
30. Tauer TP, Sherrill CD (2005) J Phys Chem A 109:10475–10478
31. Cysewski P, Czyznikowska-Balcerak Z (2005) J Mol Struct Theochem 757:29–36
32. Hunter CA, Singh J, Thornton JM (1991) J Mol Biol 218:837–846. doi:10.1016/0022-2836(91)90271-7
33. Rozas I, Alkorta I, Elguero J (2004) J Phys Chem B 108:3335–3341. doi:10.1021/jp036901m
34. Dougherty DA (1996) J Sci 271:163–168. doi:10.1126/science.271.5246.163
35. Lummis SC, Beene DL, Harrison NJ, Lester HA, Dougherty A (2005) J Chem Biol 12:993–997. doi:10.1016/j.chembiol.2005.06.012
36. Yang Z, Rodgers MT (2004) J Am Chem Soc 126:16217–16226. doi:10.1021/ja045375p
37. Sinnnokrot MO, Sherrill CD (2006) J Phys Chem A 110:10656–10668. doi:10.1021/jp0610416
38. Moller C, Plesset MS (1934) Phys Rev 46:618–622. doi:10.1103/PhysRev.46.618
39. Leininger ML, Nielsen IMB, Colvin ME, Janssen CL (2002) J Phys Chem A 106:3850–3854. doi:10.1021/jp013866f
40. Zhao Y, Truhlar DG (2004) J Phys Chem A 108:6908–6918. doi:10.1021/jp048147q
41. Stephens PJ, Devlin FJ, Chabalowski CF, Frisch MJ (1994) J Phys Chem 98:11623–11627
42. Zhao Y, Truhlar DG (2008) Acc Chem Res 41:157–167
43. Zhao Y, Truhlar DG (2006) J Chem Phys 124:224105-1–224105-6
44. Zhoa Y, Truhlar DG (2006) J Phys Chem A 110:10478–10486
45. Zhao Y, Truhlar DG (2007) J Chem Theory Comput 3:289–300
46. Grimme S (2006) J Comput Chem 27:1787–1799
47. Jureka P, Cerny J, Hobza P, Salahub DR (2007) J Comput Chem 28:555–569
48. Kolář M, Hobza P (2007) J Phys Chem A 111:5851–5854. doi:10.1021/jp071486+
49. Zhao Y, Schultz NE, Truhlar DG (2006) J Chem Theory Comput 2:364–382. doi:10.1021/ct0502763
50. Zhao Y, Truhlar DG (2006) J Phys Chem A 110:13126–13130
51. Zhao Y, Truhlar DG (2008) Theor Chem Acc 120:215–241. doi:10.1007/s00214-007-0310-x
52. Wintjens R, Biot C, Rooman M, Lievin J (2003) J Phys Chem A 107:6249–6258. doi:10.1021/jp034103q
53. Frisch MJ et al (2003) Gaussian 03 (Revision B.03). Gaussian, Inc, Pittsburgh, PA
54. Schmidt MW, Baldridge KK, Boat JA, Elbert ST, Gordon MS, Jensen JH, Koseki S, Matsunaga N, Nguyen KA, Su SJ, Windus TL, Dupuis M, Montgomery JA (1993) J Comput Chem 14:1347–1363. doi:10.1002/jcc.540141112
55. Bader RFW (1990) Oxford University Press, Oxford
56. Biegler König FW, Schönbohm J, Bayles D (2001) J Comput Chem 22:545–559. doi:10.1002/1096-987X(20010415)22:5<545::AID-JCC1027>3.0.CO;2-Y
57. Boys SB, Bernardi F (1970) Mol Phys 19:553–566. doi:10.1080/00268977000101561
58. Rozas I, Alkorta I, Elguero J (2000) J Am Chem Soc 122:11154–11161. doi:10.1021/ja0017864